

Transient Localization from the Interaction with Quantum Bosons

Hadi Rammal¹,^{ORCID} Arnaud Ralko¹,^{ORCID} Sergio Ciuchi²,^{ORCID} and Simone Fratini¹^{ORCID}

¹*Université Grenoble Alpes, CNRS, Grenoble INP, Institut Néel, 38000 Grenoble, France*

²*Dipartimento di Scienze Fisiche e Chimiche, Università dell'Aquila, Coppito-L'Aquila, Italy*



(Received 7 December 2023; accepted 22 May 2024; published 24 June 2024)

We carefully revisit the electron-boson scattering problem, going beyond weak-coupling expansions and popular semiclassical treatments. By providing numerically exact results valid at finite temperatures, we demonstrate the existence of a broad regime of electron-boson scattering where quantum localization processes become relevant despite the absence of extrinsic disorder. Localization in the Anderson sense is caused by the dynamical randomness resulting from a large thermal boson population, being, however, effective only at transient times before diffusion can set in. Compelling evidence of this transient localization phenomenon is provided by the observation of a distinctive displaced Drude peak in the optical absorption and the ensuing suppression of conductivity. Our findings identify a general route for anomalous metallic behavior that can broadly apply in interacting quantum matter.

DOI: [10.1103/PhysRevLett.132.266502](https://doi.org/10.1103/PhysRevLett.132.266502)

Introduction.—Unusual charge transport properties are both a defining feature and an open challenge in quantum materials. Bad metals exhibit anomalously large resistivities, defying the very assumptions of textbook, Bloch-Boltzmann, transport theory. Posing even more fundamental challenges, the celebrated Fermi-liquid theory of metals breaks down altogether in strange metals. Several theoretical routes are being explored, and novel concepts have been put forward to explain these anomalies. In one class of scenarios, the anomalies are ascribed to the unusual properties of the scatterers involved, that are able to overcome and replace the traditional electron-electron and electron-phonon scattering channels. Notable examples in this category include various types of critical, soft bosons appearing at quantum phase transitions or in extended critical phases [1–3], eventually leading to bad metal behavior, strange metal behavior, or both. In a second group of scenarios, it is the very existence of electronic quasiparticles that is questioned: The observed anomalies would then originate from the strange nature of the current carriers, that cannot be described as individual quasiparticles in the usual sense. Examples of these scenarios include the reported destruction of quasiparticles by strong electron-electron interactions in correlated metals at high temperatures [4–7], shifting the focus on the consequences of interaction-induced randomness [8], or more radical model descriptions where the quasiparticle concept is abandoned from the outset [9,10]. While we find this distinction useful, in principle, it should be stressed that in actual materials these two phenomena often occur together, with the emergent soft bosons also leading to the destruction of quasiparticles [11].

In this Letter, we explore a third route, where neither the scatterers nor the carriers are anomalous; what is anomalous instead is the nature of the scattering process itself, that

will eventually lead to unusual charge transport. What we propose here is that, whenever there is dynamical randomness in the problem, it might become relevant to consider the effects of such randomness in full, including the quantum localization phenomena that are traditionally associated with disordered systems.

The idea that quantum localization processes can lead to anomalous charge transport at room temperature was initiated in recent years in order to explain the puzzling properties of crystalline organic semiconductors [12–14]. There, just like in bad metals, the apparent time separating two subsequent collision events is too short to be compatible with semiclassical charge transport. The origin of the anomaly and the solution to the puzzle are now understood as follows: In molecular crystals, the intermolecular vibrations are extremely soft for structural reasons, and they are, therefore, easily thermally populated; when these incoherent vibrations couple to the electronic motion, they result in strong randomness that is able to localize the electrons *à la* Anderson, albeit only on relatively short timescales. Electronic transport is then characterized by subsequent localization and delocalization processes [15–17] that eventually lead to reduced diffusion, i.e., bad conduction. This phenomenon comes with an associated fingerprint: The electronic optical response exhibits a distinctive displaced Drude peak, providing direct evidence for localization.

Given the amount of existing knowledge on electron-phonon interactions, it came as a surprise that a previously unreported regime of electron-boson scattering could be uncovered. Even more puzzling, the latter has been shown to appear already for weak interactions, yet it had eluded even the most refined semiclassical treatments available [18], revealing the need to fully account for

the quantum nature of the electronic carriers and the interference processes associated with it.

The phenomenon described above, now known as *transient localization*, was originally found through direct time-dependent solution methods that treated the dynamic disorder classically [12]. The nature of the observed localization was then understood analytically, through a relaxation time approximation [13,14,19] building on the observation that slow dynamic scatterers should behave increasingly close to static disorder as their characteristic frequency scale approaches zero. More refined quantum-classical approaches have successfully been applied since, providing detailed, material-oriented predictions [20–24]. Yet, all these methods have major drawbacks stemming from the classical treatment of the bosons, and they could not provide a conclusive solution to the problem. Whether and how this phenomenon can be sustained when the quantum nature of the bosons is restored has, therefore, remained an open question: According to the common wisdom, quantum bosons should either bind to the charge carriers or scatter them inelastically [25], not localize them.

Hinting at the existence of transient localization beyond the classical boson limit, signatures compatible with it have been found in fully quantum numerical studies [22,26–30]. It is the purpose of the present work to demonstrate this phenomenon in an unbiased and systematic way—here, by solving exactly a paradigmatic one-dimensional model—showing how localization processes develop from electron-boson interactions through the emergence of a displaced Drude peak and a consequent suppression of the carrier diffusion.

Model and method.—We consider the Holstein model:

$$H = -t \sum_{\langle ij \rangle} c_i^\dagger c_j + \omega_0 \sum_i \left(a_i^\dagger a_i + \frac{1}{2} \right) + g \sum_i c_i^\dagger c_i (a_i^\dagger + a_i) \quad (1)$$

describing the local interaction of tight-binding electrons, c_i and c_i^\dagger at site i , with quantum bosons, a_i and a_i^\dagger , of characteristic frequency ω_0 . We define the dimensionless coupling strength $\lambda = g^2/(2t\omega_0)$ and set $\hbar = 1$. In the original electron-phonon problem, the latter represent local atomic or molecular vibrations; more generally, Eq. (1) can effectively describe the interaction with collective or critical modes emerging from electron-electron interactions. Because we aim at providing an unbiased proof of principle on the existence of localization by quantum bosons, we opt for an exact numerical solution of the model. This choice brings stringent limitations on the attainable system sizes, due to the known exponential growth of the Hilbert space (see below); for this reason, we restrict our study to one space dimension, where the attainable linear sizes are maximal and localization effects are quantitatively strongest. Beyond this practical choice, our conclusions regarding

the transient localization phenomenon *per se* will be unaffected in higher dimensions. For similar reasons, since the localization mechanism of interest here is active already at the single-electron level, we study the scattering problem defined by Eq. (1) for an individual electron, setting aside the explicit many-body renormalization (softening) of the bosons by the electronic polarization, that has been studied elsewhere [19,31], as well as the associated damping.

We solve the model Eq. (1) using the finite-temperature Lanczos method (FTLM) [32,33] on finite-size chains of length N_s , truncating the infinite Hilbert space of the bosons to a total maximum number N_{bos} of quanta on the chain (details in Supplemental Material [34]). This method provides a formally exact high-temperature expansion for both the thermodynamic quantities and dynamic correlation functions down to temperatures of the order of a fraction of t . Working at nonzero temperatures drastically reduces finite-size effects as compared with $T = 0$ exact diagonalization [33]. These are further minimized by averaging over N_ϕ twisted boundary conditions (TBCs) [35,36], increasing the effective number of allowed momenta from the nominal value N_s to $N_s \times N_\phi$. TBC sampling permits us to obtain reliable results down to the weak-coupling regime, where the discrete nature of the noninteracting spectrum on small clusters is most critical. We use $N_s = 4, 5, 6$ and $N_\phi = 40$, sufficient for convergence in the temperature range of interest.

Dynamical disorder and displaced Drude peak.—Figure 1(a) shows the regular ($\omega > 0$) part of the optical conductivity per particle calculated at different temperatures in the slow-boson (adiabatic) regime, $\omega_0/t = 0.3$, for a moderate coupling strength $\lambda = 0.3$ (see Supplemental Material [34] for details). At low temperature, $T = 0.15t < \omega_0$, the optical absorption recovers the expected weak-coupling picture [37]: The spectrum is constituted of a main absorption peak at $\omega = \omega_0$ corresponding to single-boson emission, followed by weaker shakeoff replicas at multiples of ω_0 . Upon increasing the temperature, however, the finite-frequency absorption peak is not washed out as predicted by semiclassical approaches [37]. Quite on the contrary, the peak at ω_0 shifts to higher frequencies, progressively evolving into a broader shape (see also Ref. [27]). As we show next, this indicates that the nature of the electron-boson scattering smoothly evolves from independent, one-boson emission events to a fundamentally different regime where dynamical disorder from abundant thermally excited bosons creates the conditions for localization in the Anderson sense. This should not be confused with the usual absorption peak resulting from polaron formation in the strong electron-boson coupling regime, where charge transport is instead dominated by boson-assisted hopping [25] (see Supplemental Material [34]).

To verify this hypothesis, we rewrite the harmonic Hamiltonian in first quantization as $\omega_0(a_i^\dagger a_i + 1/2) = P_i^2/2M + M\omega_0^2 X_i^2/2$ and explicitly neglect the dynamic

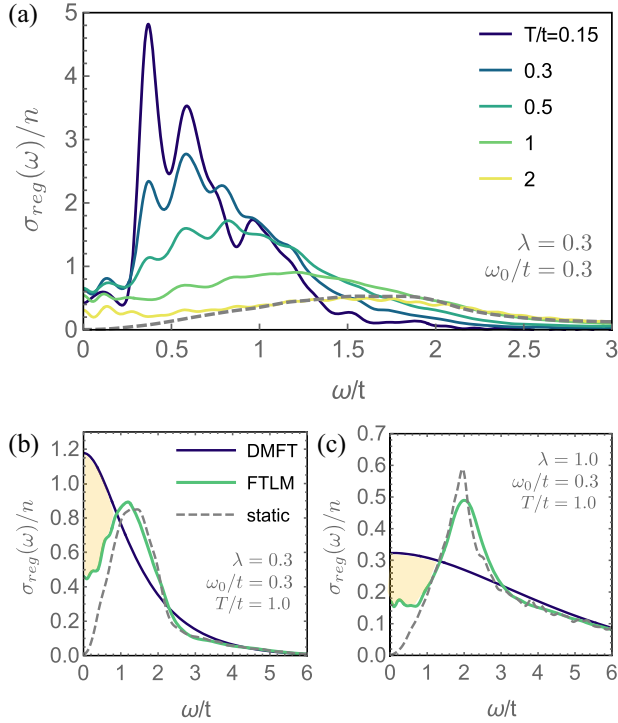


FIG. 1. (a) Regular part of the optical conductivity per particle for $\lambda = 0.3$, $\omega_0/t = 0.3$ calculated at different temperatures, expressed in units of $e^2 a^2/\hbar$, with a the lattice spacing (values $\sigma/n < 2$ imply apparent scattering times shorter than the hopping time τ^{-1} [14]). The cluster parameters are $N_s = 4$, $N_{\text{bos}} = 70$, and $N_\phi = 40$. The dashed line is the result from the static boson approximation at $T/t = 2$ (a Gaussian filter of width $\delta = 0.045t$ has been applied to all curves). The observed range of peak frequencies $\omega_L/t = 0.4$ – 2 corresponds to localization lengths $L = 1$ – 2.2 , consistently smaller than the system size. (b) Enlargement of the FTLM data at $T/t = 1.0$ compared with the DMFT result and the static boson approximation. (c) Similar to (b), at $\lambda = 1.0$. In (b) and (c), the filter is $\delta = 0.08t$.

part, formally taking the static boson limit $M \rightarrow \infty$, $\omega_0 \rightarrow 0$ with $M\omega_0^2 = \text{const}$ [19]. The interaction part then becomes $\sum_i (gX_i) c_i^\dagger c_i$, resulting in a one-body problem with disordered site energies $\epsilon_i = gX_i$ [the latter obey a Gaussian distribution of variance $\Delta = \sqrt{2\lambda\omega_0/\tanh(\omega_0/2T)}$, which follows directly from the properties of the harmonic oscillator]. The corresponding optical conductivity is reported as a gray dashed line in Fig. 1(a) for $T/t = 2$: It shows a disorder-induced localization peak at a frequency $\omega_L \simeq 2t/L^2$ [13,14,19], corresponding to the typical level spacing in a localization well of size L .

A more stringent comparison with the static boson result is provided in Figs. 1(b) and 1(c) for moderate ($\lambda = 0.3$) and strong ($\lambda = 1.0$) electron-boson interactions. In both cases, the shape and position of the finite-frequency peak obtained in the fully quantum FTLM treatment coincide with the result of the static disorder problem at all frequencies $\omega \gtrsim \omega_0$, i.e., whenever the electrons are driven

at a frequency that is faster than the bosons. The compelling agreement observed on the localization-induced peak demonstrates that thermally populated bosons are able to localize the electronic wave function even though there is no explicit random term in Eq. (1). The fact that the conductivity is instead not completely suppressed when $\omega < \omega_0$ indicates that the quantum interference processes at play here are only transient, being eventually destroyed at times longer than ω_0^{-1} . A detailed discussion of the dc limit $\omega \rightarrow 0$ is provided in the second part of this Letter.

Conditions for transient localization and one-parameter scaling.—Localization originates from quantum interference effects not contained in semiclassical descriptions of electron transport. Remarkably, the failure in capturing this phenomenon does not spare even modern sophisticated treatments such as dynamical mean field theory (DMFT) or other large- N -based approaches [8] that rely on self-averaging assumptions and, therefore, disregard nonlocal interferences by construction; in diagrammatic terms, current vertex corrections are ignored [5]. This is illustrated in Figs. 1(b) and 1(c), where alongside the FTLM and static boson results we report the optical spectra calculated within single-site DMFT [18], showing no sign of a displaced Drude peak (DDP) as expected.

To analyze the phenomenon further, we report in Fig. 2(a) the evolution of the peak frequency with

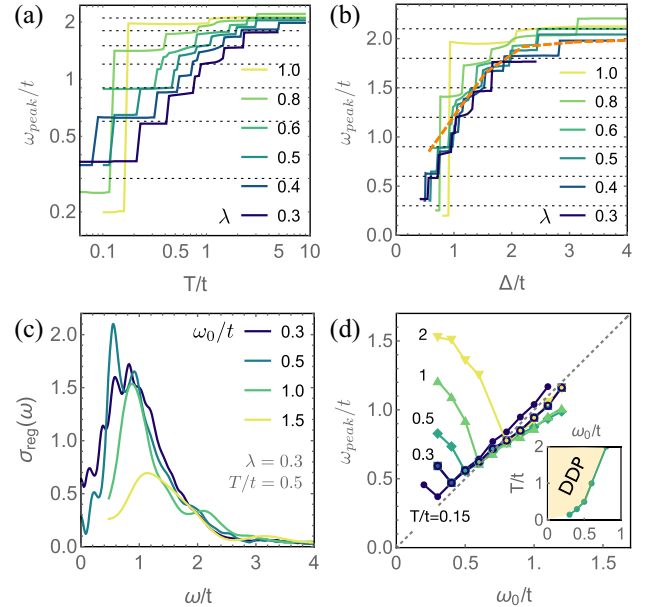


FIG. 2. Peak position (a) as a function of T and (b) as a function of dynamical disorder Δ , for $\omega_0 = 0.3$ and different values of λ . Dotted lines indicate multiples of ω_0 . The dashed line is the result from the static boson limit for $\lambda = 0.3$. (c) Spectra at $\lambda = 0.3$, $T/t = 0.5$, and different ω_0 , with $\delta = 0.15\omega_0$. The low-frequency part becomes inaccessible at large ω_0 ; see Supplemental Material [34]. (d) Peak position vs ω_0 at different T ; the dashed line is $\omega_{\text{peak}} = \omega_0$. The inset shows the temperature range of existence of the DDP as extracted from the data in the main panel.

temperature at different values of the electron-boson coupling strength. In all cases, the peak frequency increases monotonically with T , and it also shows an overall increase with λ at fixed T . This behavior can be collapsed onto a single curve when expressed as a function of the variance Δ of the dynamical bosonic disorder, which is illustrated in Fig. 2(b). The superimposed steps observed at multiples of ω_0 originate from the multiboson fine structure seen in Fig. 1(a).

Implicit in the arguments given in the preceding paragraphs, two conditions must be met for the emergence of a localization-induced DDP. (i) The bosons must be largely—and incoherently—populated, which requires that T is larger than the Debye temperature of the bosons. For weak interactions, this translates into $k_B T \gtrsim \hbar \omega_0$, but the DDP can, in principle, be sustained down to lower temperatures if the boson frequency is itself renormalized by interactions, which is known to happen when interactions are strong [19]. (ii) The dynamics of boson-induced disorder, governed by the timescale ω_0^{-1} , must be slower than the characteristic time of localization, ω_L^{-1} , i.e., $\omega_L > \omega_0$: Only in this case can the localization processes build up in the disordered environment created by the bosons, that the electrons will see as quasistatic.

To illustrate these conditions, Fig. 2(c) shows the evolution of the optical absorption upon varying ω_0 at a fixed temperature $T = 0.5t$. For $\omega_0 < T$, the spectrum displays a disorder-induced DDP, here located at $\omega_L \simeq 0.8t$ (the same data as in Fig. 1). Upon increasing ω_0 (reducing T/ω_0), the DDP initially softens as boson coherence builds up, effectively reducing the amount of thermal disorder. As soon as ω_L hits ω_0 , the peak bounces back and hardens again, following $\omega_{\text{peak}} = \omega_0$: The disorder-induced DDP has disappeared in favor of a more conventional single-boson peak. The same evolution is actually observed at all temperatures, starting from different initial values of ω_L in the limit $\omega_0 \rightarrow 0$ [Fig. 2(d)].

Suppression of the conductivity and validation of the transient localization formula.—We finally come to the key point concerning charge transport: The suppression of low-frequency spectral weight that accompanies the formation of the displaced Drude peak extends down to $\omega = 0$, causing a suppression of the electrical conductivity (an increase in resistivity) as compared to semiclassical estimates. This is illustrated in Fig. 3, showing the temperature dependence of the resistivity at $\omega_0/t = 0.3$ for $\lambda = 0.3$ (a) and $\lambda = 1.0$ (b). Each data point has been obtained by extrapolating to the $N_{\text{bos}} \rightarrow \infty$ limit for fixed cluster size and then checking that the result is independent on N_s (cf. Supplemental Material [34]), being, therefore, representative of the thermodynamic limit. The calculated resistivity is systematically larger than the DMFT result, due to quantum localization corrections.

Figure 3(a) reveals an approximately T -linear resistivity in the moderate electron-boson coupling regime (dashed

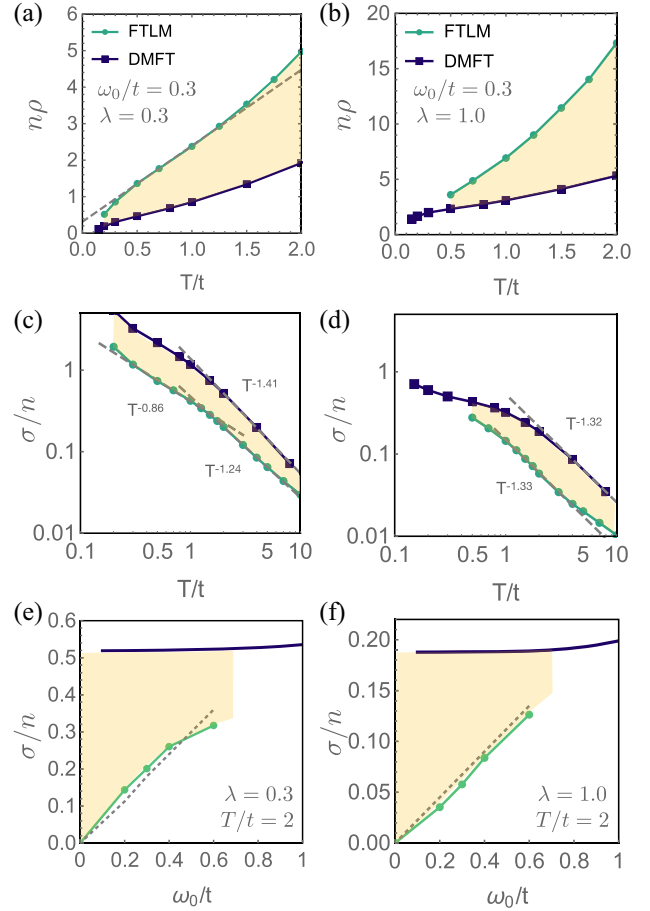


FIG. 3. (a),(b) Temperature dependence of the resistivity per particle, calculated by extrapolating the FTLM data to $N_{\text{bos}} = \infty$ at $N_s = 4$ for $\omega_0/t = 0.3$, $\lambda = 0.3$ (a), and $\lambda = 1.0$ (b) ($\delta = 0.08t$). The shaded area represents the increase in resistivity caused by quantum localization processes. (c),(d) Conductivity per particle, plotted in log scale to highlight the power-law dependence at high T (labels). (e),(f) Dependence of the conductivity on the bosonic scale ω_0 at $T = 2$ (e) for $\lambda = 0.3$ and (f) for $\lambda = 1.0$. The dashed line is the prediction of the transient localization formula based on the observed DDP position (see the text).

line). The log-scale plots in Figs. 3(c) and 3(d) provide more precise estimates of the power-law dependence of the conductivity. Comparison with DMFT shows that localization corrections amount to a mostly T -independent suppression factor, only weakly affecting the power-law exponent.

We now show how the reduction of the conductivity depends on the bosonic scale ω_0 . Charge diffusion is completely suppressed when $\omega_0 = 0$ (full Anderson localization), while in the opposite limit localization effects are destroyed when $\omega_0 > (T, \omega_L)$, as discussed already. The conductivity in the available range of ω_0 , reported in Figs. 3(e) and 3(f), is compatible with interpolating between full localization and the semiclassical DMFT result. The suppression factor introduced by localization

is not only T independent, as shown in the preceding paragraph, but also λ independent, being, therefore, primarily governed by the ratio ω_0/t .

Finally, the numerical data presented here quantitatively validate the relaxation time approximation that was originally introduced to describe charge transport in the transient localization regime [13]. Following early ideas by Gogolin and Thouless [15–17], it was argued that in this regime the mobility $\mu = \sigma/ne$ should follow $\mu_{\text{TL}} = (e/k_B T)L^2/2\tau_0$, with τ_0 the typical timescale of the bosonic fluctuations, instead of the usual Drude expression $\mu = e\tau/m$. By extracting the localization length $L = \sqrt{2t/\omega_L}$ from the position of the DDP, we find that the TL formula is in excellent agreement with the numerical results if we set $\tau_0^{-1} = \alpha\omega_0$ with $\alpha = 1/2.2$ as in Ref. [38].

Concluding remarks.—We conclude by highlighting two concepts that could be of relevance in quantum materials and that follow directly from the results presented in this work. First, our findings unequivocally demonstrate that localization effects can arise as a general consequence of dynamical disorder. This was illustrated here in a paradigmatic model for electron-boson interactions, yet the potential implications of the phenomenon are broader: Collective excitations resulting from many-body interactions and critical modes near quantum phase transitions are two examples of bosonic degrees of freedom that are commonly found in quantum matter, that are intrinsically soft and could, therefore, cause quantum localization analogous to that described here. We advocate that any emergent randomness in interacting electron systems [8] should be taken at face value, especially in low dimensions, without disregarding the quantum processes generally associated with Anderson localization. The latter would instead be entirely missed by self-averaging theories such as dynamical mean field theory [5,18,37] and other large- N treatments [8].

Second, it is often assumed that quantum localization corrections are relevant only at very low temperatures, while they can be ignored otherwise. Our results demonstrate that the opposite is true whenever the randomness causing localization originates from dynamical bosonic fluctuations: In this case, the equipartition principle dictates that random fluctuations will grow with temperature, overcoming the dephasing effects driven by the temperature itself. Theory shows that localization processes can develop from electron-boson interactions rather than being washed out by them. From an experimental standpoint, we hope that our findings will stimulate a critical reassessment of the widely observed displaced Drude peaks in a variety of quantum materials [39–45].

S. C. acknowledges funding from NextGenerationEU National Innovation Ecosystem Grant No. ECS00000041-VITALITY-CUP E13C22001060006.

- [1] A. J. Millis, Effect of a nonzero temperature on quantum critical points in itinerant fermion systems, *Phys. Rev. B* **48**, 7183 (1993).
- [2] H. v. Löhneysen, A. Rosch, M. Vojta, and P. Wölfle, Fermi-liquid instabilities at magnetic quantum phase transitions, *Rev. Mod. Phys.* **79**, 1015 (2007).
- [3] C. Collignon, P. Bourges, B. Fauqué, and K. Behnia, Heavy nondegenerate electrons in doped strontium titanate, *Phys. Rev. X* **10**, 031025 (2020).
- [4] X. Deng, J. Mravlje, R. Žitko, M. Ferrero, G. Kotliar, and A. Georges, How bad metals turn good: Spectroscopic signatures of resilient quasiparticles, *Phys. Rev. Lett.* **110**, 086401 (2013).
- [5] J. Vučičević, J. Kokalj, R. Žitko, N. Wentzell, D. Tanasković, and J. Mravlje, Conductivity in the square lattice Hubbard model at high temperatures: Importance of vertex corrections, *Phys. Rev. Lett.* **123**, 036601 (2019).
- [6] E. W. Huang, R. Sheppard, B. Moritz, and T. P. Devereaux, Strange metallicity in the doped Hubbard model, *Science* **366**, 987 (2019).
- [7] S. Ciuchi and S. Fratini, Strange metal behavior from incoherent carriers scattered by local moments, *Phys. Rev. B* **108**, 235173 (2023).
- [8] D. Chowdhury, A. Georges, O. Parcollet, and S. Sachdev, Sachdev-Ye-Kitaev models and beyond: Window into non-Fermi liquids, *Rev. Mod. Phys.* **94**, 035004 (2022).
- [9] M. Čubrović, J. Zaanen, and K. Schalm, String theory, quantum phase transitions, and the emergent Fermi liquid, *Science* **325**, 439 (2009).
- [10] S. A. Hartnoll, A. Lucas, and S. Sachdev, *Sachdev-Ye-Kitaev Models and Beyond: Window into Non-Fermi Liquids* (MIT Press, Cambridge, MA, 2018).
- [11] S. Caprara, C. D. Castro, G. Mirarchi, G. Seibold, and M. Grilli, Dissipation-driven strange metal behavior, *Commun. Phys.* **5**, 10 (2022).
- [12] A. Troisi and G. Orlandi, Charge-transport regime of crystalline organic semiconductors: Diffusion limited by thermal off-diagonal electronic disorder, *Phys. Rev. Lett.* **96**, 086601 (2006).
- [13] S. Ciuchi, S. Fratini, and D. Mayou, Transient localization in crystalline organic semiconductors, *Phys. Rev. B* **83**, 081202(R) (2011).
- [14] S. Fratini, D. Mayou, and S. Ciuchi, The transient localization scenario for charge transport in crystalline organic materials, *Adv. Funct. Mater.* **26**, 2292 (2016).
- [15] A. Gogolin, V. Mel’nikov, and E. Rashba, Conductivity in a disordered one-dimensional system induced by electron-phonon interaction, *Sov. J. Exp. Theor. Phys.* **42**, 168 (1975).
- [16] A. Gogolin, V. Mel’nikov, and E. I. Rashba, Effect of dispersionless phonons on the kinetics of electrons in one-dimensional conductors, *Sov. J. Exp. Theor. Phys.* **45**, 330 (1977).
- [17] D. Thouless, The effect of inelastic electron scattering on the conductivity of very thin wires, *Solid State Commun.* **34**, 683 (1980).
- [18] S. Fratini and S. Ciuchi, Bandlike motion and mobility saturation in organic molecular semiconductors, *Phys. Rev. Lett.* **103**, 266601 (2009).

- [19] S. Fratini and S. Ciuchi, Displaced Drude peak and bad metal from the interaction with slow fluctuations, *SciPost Phys.* **11**, 39 (2021).
- [20] S. Fratini, S. Ciuchi, D. Mayou, G. T. de Laissardière, and A. Troisi, A map of high-mobility molecular semiconductors, *Nat. Mater.* **16**, 998 (2017).
- [21] S. Giannini, A. Carof, M. Ellis, H. Yang, O. G. Ziogos, S. Ghosh, and J. Blumberger, Quantum localization and delocalization of charge carriers in organic semiconducting crystals, *Nat. Commun.* **10**, 3843 (2019).
- [22] W. Li, J. Ren, and Z. Shuai, A general charge transport picture for organic semiconductors with nonlocal electron-phonon couplings, *Nat. Commun.* **12**, 4260 (2021).
- [23] S. Giannini, L. Di Virgilio, M. Bardini, J. Hausch, J. J. Geuchies, W. Zheng, M. Volpi, J. Elsner, K. Broch, Y. H. Geerts, F. Schreiber, G. Schweicher, H. I. Wang, J. Blumberger, M. Bonn, and D. Beljonne, Transiently delocalized states enhance hole mobility in organic molecular semiconductors, *Nat. Mater.* **22**, 1361 (2023).
- [24] Z. Shuai, Faster holes by delocalization, *Nat. Mater.* **22**, 1277 (2023).
- [25] G. D. Mahan, *Many-Particle Physics* (Kluwer Academic/Plenum, New York, 2000).
- [26] G. Schubert, G. Wellein, A. Weisse, A. Alvermann, and H. Fehske, Optical absorption and activated transport in polaronic systems, *Phys. Rev. B* **72**, 104304 (2005).
- [27] A. S. Mishchenko, N. Nagaosa, G. D. Filippis, A. de Candia, and V. Cataudella, Mobility of Holstein polaron at finite temperature: An unbiased approach, *Phys. Rev. Lett.* **114**, 146401 (2015).
- [28] G. D. Filippis, V. Cataudella, A. S. Mishchenko, A. N. Nagaosa, A. Fierro, and A. de Candia, Crossover from super-to-subdiffusive motion and memory effects in crystalline organic semiconductors, *Phys. Rev. Lett.* **114**, 086601 (2015).
- [29] D. Jansen and F. Heidrich-Meisner, Thermal and optical conductivity in the holstein model at half filling and finite temperature in the Luttinger-liquid and charge-density-wave regime, *Phys. Rev. B* **108**, L081114 (2023).
- [30] V. Janković, Holstein polaron transport from numerically “exact” real-time quantum dynamics simulations, *J. Chem. Phys.* **159**, 094113 (2023).
- [31] D. Di Sante, S. Fratini, V. Dobrosavljević, and S. Ciuchi, Disorder-driven metal-insulator transitions in deformable lattices, *Phys. Rev. Lett.* **118**, 036602 (2017).
- [32] J. Jaklič and P. Prelovšek, Lanczos method for the calculation of finite-temperature quantities in correlated systems, *Phys. Rev. B* **49**, 5065 (1994).
- [33] P. Prelovšek and J. Bonča, Ground state and finite temperature Lanczos methods, in *Strongly Correlated Systems: Numerical Methods*, edited by A. Avella and F. Mancini (Springer, Berlin, 2013), pp. 1–30.
- [34] See Supplemental Material at <http://link.aps.org/supplemental/10.1103/PhysRevLett.132.266502> for details on the numerical method and its implementation.
- [35] D. Poilblanc, Twisted boundary conditions in cluster calculations of the optical conductivity in two-dimensional lattice models, *Phys. Rev. B* **44**, 9562 (1991).
- [36] C. Gros, The boundary condition integration technique: Results for the Hubbard model in 1D and 2D, *Z. Phys. B Condens. Matter* **86**, 359 (1992).
- [37] S. Fratini and S. Ciuchi, Optical properties of small polarons from dynamical mean-field theory, *Phys. Rev. B* **74**, 075101 (2006).
- [38] S. Fratini and S. Ciuchi, Dynamical localization corrections to band transport, *Phys. Rev. Res.* **2**, 013001 (2020).
- [39] S. Fratini, K. Driscoll, S. Ciuchi, and A. Ralko, A quantum theory of the nearly frozen charge glass, *SciPost Phys.* **14**, 124 (2023).
- [40] K. Takenaka, M. Tamura, N. Tajima, H. Takagi, J. Nohara, and S. Sugai, Collapse of coherent quasiparticle states in $\theta - (\text{BEDT} - \text{TTF})_2\text{I}_3$ observed by optical spectroscopy, *Phys. Rev. Lett.* **95**, 227801 (2005).
- [41] A. Pustogow, Y. Saito, A. Löhle, M. S. Alonso, A. Kawamoto, V. Dobrosavljević, M. Dressel, and S. Fratini, Rise and fall of Landau’s quasiparticles while approaching the Mott transition, *Nat. Commun.* **10**, 41467 (2021).
- [42] S. Lupi, P. Calvani, M. Capizzi, and P. Roy, Evidence of two species of carriers from the far-infrared reflectivity of $\text{Bi}_2\text{Sr}_2\text{CuO}_6$, *Phys. Rev. B* **62**, 12418 (2000).
- [43] A. Biswas, O. Iakutkina, Q. Wang, H. C. Lei, M. Dressel, and E. Uykur, Spin-reorientation-induced band gap in Fe_3Sn_2 : Optical signatures of Weyl nodes, *Phys. Rev. Lett.* **125**, 076403 (2020).
- [44] Y. S. Lee, J. Yu, J. S. Lee, T. W. Noh, T.-H. Gimm, H.-Y. Choi, and C. B. Eom, Non-Fermi liquid behavior and scaling of the low-frequency suppression in the optical conductivity spectra of CaRuO_3 , *Phys. Rev. B* **66**, 041104(R) (2002).
- [45] N. L. Wang, P. Zheng, D. Wu, Y. C. Ma, T. Xiang, R. Y. Jin, and D. Mandrus, Infrared probe of the electronic structure and charge dynamics of $\text{Na}_{0.7}\text{CoO}_2$, *Phys. Rev. Lett.* **93**, 237007 (2004).